Available online at www.sciencedirect.com

ScienceDirect

Journal of Computational and Applied Mathematics 198 (2007) 268–286

JOURNAL OF COMPUTATIONAL AND APPLIED MATHEMATICS

www.elsevier.com/locate/cam

A fourth-order compact ADI method for solving two-dimensional unsteady convection–diffusion problems

Z.F. Tian[a, b, *], Y.B. Ge[b]

[a] *Shanghai Institute of Applied Mathematics and Mechanics, Shanghai University, Shanghai 200072, PR China*
[b] *Institute of Applied Mathematics and Engineering Mechanics, Ningxia University, Yinchuan, Ningxia 750021, PR China*

Received 6 August 2005; received in revised form 5 December 2005

Abstract

In this article, an exponential high-order compact (EHOC) alternating direction implicit (ADI) method, in which the Crank–Nicolson scheme is used for the time discretization and an exponential fourth-order compact difference formula for the steady-state 1D convection–diffusion problem is used for the spatial discretization, is presented for the solution of the unsteady 2D convection–diffusion problems. The method is temporally second-order accurate and spatially fourth order accurate, which requires only a regular five-point 2D stencil similar to that in the standard second-order methods. The resulting EHOC ADI scheme in each ADI solution step corresponds to a strictly diagonally dominant tridiagonal matrix equation which can be inverted by simple tridiagonal Gaussian decomposition and may also be solved by application of the one-dimensional tridiagonal Thomas algorithm with a considerable saving in computing time. The unconditionally stable character of the method was verified by means of the discrete Fourier (or von Neumann) analysis. Numerical examples are given to demonstrate the performance of the method proposed and to compare mostly it with the high order ADI method of Karaa and Zhang and the spatial third-order compact scheme of Note and Tan.

Keywords: Higher-order compact scheme; Unsteady; Convection–diffusion; Alternating direction implicit method

1. Introduction

The convection–diffusion equation always attracts research interests for its academic significance as well as its relevance to broad range of practical applications, especially those involving fluid flow and heat transfer. Numerical prediction of the convection–diffusion equation plays a very important role in computational fluid dynamics (CFD) to simulate flow problems. Therefore, accurate and stable difference representations of the convection–diffusion equations are of vital importance.

In this paper, we consider the following unsteady 2D convection–diffusion equation:

$$\frac{\partial u}{\partial t} - a\frac{\partial^2 u}{\partial x^2} - b\frac{\partial^2 u}{\partial y^2} + p\frac{\partial u}{\partial x} + q\frac{\partial u}{\partial y} = S, \quad (x, y, t) \in \Omega \times (0, T] \tag{1}$$

* Corresponding author.
E-mail address: zftian@nxu.edu.cn (Z.F. Tian).

0377-0427/$ - see front matter © 2005 Elsevier B.V. All rights reserved.
doi:10.1016/j.cam.2005.12.005

with initial condition

$$u(x, y, 0) = u_0(x, y), \quad (x, y) \in \Omega \tag{2}$$

and Dirichlet boundary condition

$$u(x, y, t) = g(x, y, t), \quad (x, y, t) \in \partial\Omega \times (0, T], \tag{3}$$

where Ω is a rectangular domain in $\mathbb{R}^2$, $\partial\Omega$ is the boundary of Ω, $(0, T]$ is the time interval, and u_0, g and the source term $S(x, y, t)$ are given sufficiently smooth functions (without loss of generally, we consider $S \equiv 0$ in the following), and $u(x, y, t)$ may represent heat, vorticity, etc. In Eq. (1), p and q are constant, convective velocities and a and b are constant, positive diffusion coefficients in the x- and y-direction, respectively.

Model equation (1), rewritten for the two-dimensional steady-state case, becomes

$$-a\frac{\partial^2 u}{\partial x^2} - b\frac{\partial^2 u}{\partial y^2} + p\frac{\partial u}{\partial x} + q\frac{\partial u}{\partial y} = S(x, y), \tag{4}$$

where S is a sufficient smooth function with respect to x and y. Eqs. (1) and (4) can describe the convection and diffusion of various physical quantities, e.g. mass, momentum and energy, etc. It is encountered in many fields of engineering and science such as heat transfer, fluid flows and the groundwater pollution problems and chemical separation processes [21,18,1].

A reliable numerical model must have the ability to simulate transport phenomenon accurately while being able to suppress numerical instability arising in the course of discretization. Classical spatial discretization, such as the second-order central difference (CD) scheme or the first-order upwind difference (UD) scheme, fail to approach the exact solution of (1) or (4), unless a large number of mesh points is used. For many application problems it is desirable to use higher order numerical methods to obtain accurate solution.

In the context of high order finite differences, compact finite difference methods feature high-order accuracy and smaller stencils. Recently, there has been a renewed interest in the development and application of compact finite difference methods for the numerical solution of the convection–diffusion equations and the Navier–Stokes equations [10,8,25,14,31,28,29,15]. It is evident that they are not only accurate and cost effective but also easier treatment of boundary conditions. For steady-state 2D convection diffusion problems, Gupta et al. [10] employed series expansions to the differential equation to develop a fourth-order nine-point compact FD formula, which was shown to be able to yield highly accurate numerical solutions. Similar higher-order compact have been developed by others authors [25,14]. Dennis and Hudson [8] derived the same scheme as in Ref. [10] using another approach.

Instead of the separate treatment of convection and diffusion terms, one may consider these two terms simultaneously by incorporating a local exact solution for the convection–diffusion equations with the finite computational cells. This approach results in the so-called exponential difference (ED) scheme since the influence coefficients are connected to exponential functions [5,15,6,7,24,22,2,9,23,3]. This scheme has the noteworthy features that can be simplified to the CD scheme in the case of low flow velocity or sufficiently refined grid and to the UD scheme in the high velocity condition. Upwind convection effects are inherently considered in the exponential functions. The ED scheme of the convection–diffusion equation was first introduced by Allen and Southwell [5] to solve the second-order partial differential equation governing the transport of vorticity. The methods were analyzed by Dennis [6,7] who found that the schemes were superior to the standard difference procedures and also developed several extensions of the methods. Spalding [24] and Roscoe [22] had independently developed similar exponential-type schemes. Roscoe called these exponential-type schemes as unified difference schemes and used them for solving the Navier–Stokes equations [22]. MacKinnon and Johnson [15] also developed a compact fourth-order FD scheme. By using the governing differential equation to represent the leading truncation terms, higher-order derivatives were replaced by lower-order derivatives and then approximated on a compact stencil. Afterwards, a perturbational h^4 compact exponential finite difference scheme was developed by Chen et al. [2] for the convection–diffusion equations and numerical examples including one- to three-dimensional problems were solved to illustrate the behavior of the developed exponential schemes.

As stated above, the high-order compact numerical solutions of the steady-state 2D convection diffusion problems have been studied extensively in numerous papers. In contrast, the high-order compact methods of unsteady 2D convection–diffusion equations have not been studied to the same extent [11,17,12,13]. It must be noted, however, that several compact, 3-point, finite difference methods which are fourth-order accurate in space were developed for

the unsteady 1D convection–diffusion problems. Hirsh [11] proposed a 3-point, fourth-order compact finite difference method for the one-dimensional problems which consider the dependent variable and its first- and second-order spatial derivatives as unknowns. Thus, the one-dimensional convection–diffusion problem would required a $3N \times 3N$ matrix solve, where N is the total number grid points. Ciment et al. [3] presented a fourth-order three-point operator compact implicit (OCI) scheme for the 1D parabolic problem. It is shown that this standard OCI scheme has formal cell Reynolds number limitations. Noye and Tan [16] developed a third-order semi-implicit finite difference method for solving the unsteady one-dimensional convection–diffusion equation. This scheme is very accurate and computationally fast, but is conditionally stable. Rigal [20] developed a class three-point spatially order 4 and temporally order 2 compact finite difference scheme. This general class of finite difference scheme includes several schemes independently proposed by different authors. In recent year, Spotz and Carey [26] extended their previous approaches for steady high-order compact (HOC) difference methods [25] to the 1D unsteady convection–diffusion equations with variable coefficients. The proposed method is also conditionally stable. For unsteady 2D convection–diffusion problems, Hirsh [11] and Ciment et al. [3] have discussed compact difference schemes which are conditionally stable and of fourth-order in space and second-order in time. Noye and Tan [16] developed a third-order nine-point HOC implicit scheme for the unsteady 2D problems with constant coefficients. The scheme is spatially third-order accurate and temporally second-order accurate, and has a large stability region. Based on the work in [26], Kalita et al. derived a class of HOC schemes for the 2D unsteady convection–diffusion equation with variable convection coefficients [12]. Recently, Karra and Zhang [13] developed a HOC ADI method for solving 2D unsteady convection diffusion problems. The method, in which the Crank-Nicolson scheme is used for the time discretization and a polynomial fourth-order compact difference formula for the unsteady 1D convection–diffusion problem is used for the spatial discretization, is second-order in time and fourth-order in space and unconditionally stable, and allows a considerable saving in computing time. We are interested in ADI methods since they are highly efficient procedures for solving parabolic and hyperbolic initial-boundary value problems [4,27]. As it was shown in [27], the efficient of ADI methods is based on reducing problems in several space variables to collections of one-dimensional problems and only requiring to solve tri-diagonal matrices.

This paper is primarily aimed at introducing an exponential high order ADI method with high efficiency, accuracy, stability and robustness for solving unsteady 2D convection–diffusion equations. The Crank–Nicolson method is used for the time discretization and an exponential fourth-order compact difference formula for the steady-state 1D convection–diffusion problem is used for the space discretization. In comparison to the HOC ADI method proposed in [13], the derivation of the EHOC method is based on an exponential fourth-order compact difference operator for the spatial approximation and an exponential difference operator for the temporal approximation. The resulting EHOC ADI finite difference equation in each ADI solution step corresponds to a strictly diagonally dominant tridiagonal matrix which can be directly inverted by simple tridiagonal Gaussian decomposition and may also be solved by application of the one-dimensional tridiagonal Thomas algorithm with a considerable saving in computing time.

The rest of the present paper is organized as follows. In the next section, we first introduce an approach to designing high order ADI finite difference method with exponential coefficients for solving unsteady 2D convection diffusion equation (1). The linear of Fourier (or von Neumann) stability of the proposed EHOC ADI method is analyzed in Section 3. In Section 4, numerical experiments for three test problems are performed to validate the feasibility of the proposed methods. Finally, Section 5 is devoted to some concluding remarks.

2. Exponential compact high-order ADI finite difference method

To introduce the basic idea, let us start from the elementary, steady, 1D convection diffusion equation

$$-au_{xx} + pu_x = f, \tag{5}$$

where a is the positive constant conductivity, p is the constant convective velocity, f is a sufficiently smooth function of x. Consider the finite difference scheme for Eq. (5) with constant convection coefficient at a grid point x_i as

$$-\alpha\delta_x^2 u_i + c\delta_x u_i = \alpha_0 f_i + \alpha_1 f_{xi} + \alpha_2 f_{xxi}, \tag{6}$$

where δ_x^2 and δ_x are the second- and first-order central difference operators. In order to determine the parameters α, α_0, α_1, α_2 and c, let us rewrite Eq. (6) as

$$-\alpha\delta_x^2 u_i + c\delta_x u_i = \alpha_0(-au_{xx} + pu_x)_i + \alpha_1(-au_{xx} + pu_x)_{xi} + \alpha_2(-au_{xx} + pu_x)_{xxi}. \tag{7}$$

The parameters α, α_0, α_1, α_2 and c in Eq. (7) are determined by requiring local exactness on a collection of functions of the type $\{1, x, e^{(cx)/a}, x^2, x^3\}$. Thus, the following exponential approximation be obtained:

$$(-\alpha\delta_x^2 + p\delta_x)u_i = (1 + \alpha_1\eth_x + \alpha_2\eth_x^2)f_i, \tag{8}$$

where $\eth_x$ and $\eth_x^2$ are the first- and second-order differential operators with respect to x, h_x is the mesh size, and

$$\alpha = \begin{cases} \dfrac{ph_x}{2}\coth\left(\dfrac{ph_x}{2a}\right), & p \neq 0, \\ a, & p = 0, \end{cases} \quad \alpha_1 = \begin{cases} \dfrac{a-\alpha}{p}, & p \neq 0, \\ 0, & p = 0, \end{cases} \quad \alpha_2 = \begin{cases} \dfrac{a(a-\alpha)}{p^2} + \dfrac{h_x^2}{6}, & p \neq 0, \\ \dfrac{h_x^2}{12}, & p = 0. \end{cases} \tag{9}$$

Clearly, Eq. (8) gives rise to a diagonally dominant tri-diagonal system of equations. It is interesting to note that the exponential compact finite difference (8) for the Eq. (5) is equivalent to the standard second-order central FD formula applied to the following equation:

$$-\alpha u_{xx} + pu_x = f + \alpha_1 f_x + \alpha_2 f_{xx}. \tag{10}$$

We see that Eq. (10) is a perturbation of Eq. (5) in the sense that an artificial diffusion coefficient $a[\frac{ph_x}{2a}\coth(\frac{ph_x}{2a}) - 1]$ and an artificial source term $\alpha_1 f_x + \alpha_2 f_{xx}$ have been added.

Straightforwardly calculating the right-hand side of Eq. (8) and using Taylor-series expansions and rearranging it, we obtain the following modified differential equation corresponding to the (8):

$$-au_{xx} + pu_x = f_i + \left(\frac{\alpha h_x^2}{12} - \alpha_2 a\right)\eth_x^4 u_i - \frac{ph_x^4}{120}\eth_x^5 u_i + \frac{\alpha h_x^4}{360}\eth_x^6 u_i + \mathrm{O}(h_x^6), \tag{11}$$

where $\eth_x^n$ is the nth-order exact derivative operator with respect to x. Using again Taylor-series expansions, we have

$$\alpha = a + \frac{p^2h_x^2}{12a} - \frac{p^4h_x^4}{720a^3} + \mathrm{O}(h_x^6), \quad \alpha_2 = \frac{h_x^2}{12} + \frac{p^2h_x^4}{720a^2} + \mathrm{O}(h_x^6). \tag{12}$$

Combining (11) and (12), yields

$$-au_{xx} + pu_x = f_i + \left(\frac{p^2}{180}\eth_x^4 u_i - \frac{p}{120}\eth_x^5 u_i + \frac{a}{360}\eth_x^6 u_i\right)h_x^4 + \mathrm{O}(h_x^6). \tag{13}$$

Eq. (13) shows that difference formula (8) is $\mathrm{O}(h_x^4)$ accurate at the grid points while maintaining a compact three-point stencil. Notice that differencing of the derivatives of f may be used in (8) while still maintaining overall $\mathrm{O}(h_x^4)$ accuracy on three-point stencil. Eq. (8) can be formulated symbolically as

$$(1 + \alpha_1\delta_x + \alpha_2\delta_x^2)^{-1}(-\alpha\delta_x^2 + p\delta_x)u_i = f_i. \tag{14}$$

Here the operator $(1 + \alpha_1\delta_x + \alpha_2\delta_x^2)^{-1}$ has symbolic meaning only.

Actually, the symbolic high-order compact operator approximations for first- and second-partial derivative have been used, by several authors, to derive higher order compact schemes for numerical approximation of transport problems involving convective and diffusive processes [14,31,28,11,13]. Eq. (13) shows that, when applied difference operator $(1 + \alpha_1\delta_x + \alpha_2\delta_x^2)^{-1}(-\alpha\delta_x^2 + p\delta_x)$ to differential operator $-a\eth_x^2 + p\eth_x$, the proposed scheme (8) for the steady convection–diffusion equation (5) is an exponential fourth order compact approximation. An analogous symbolic fourth order compact approximation operator can also be obtained for the y variable.

For convenience, we define several finite difference operators

$$L_x = 1 + \alpha_1\delta_x + \alpha_2\delta_x^2, \quad A_x = -\alpha\delta_x^2 + p\delta_x,$$
$$L_y = 1 + \beta_1\delta_y + \beta_2\delta_y^2, \quad A_y = -\beta\delta_y^2 + q\delta_y,$$

where δ_y and δ_y^2 are the first- and second-order central difference operators in the y-direction, and

$$\beta = \begin{cases} \dfrac{qh_y}{2}\coth\left(\dfrac{qh_y}{2b}\right), & q \neq 0, \\ b, & q = 0, \end{cases} \quad \beta_1 = \begin{cases} \dfrac{b-\beta}{q}, & q \neq 0, \\ 0, & q = 0, \end{cases} \quad \beta_2 = \begin{cases} \dfrac{b(b-\beta)}{q^2} + \dfrac{h_y^2}{6}, & q \neq 0, \\ \dfrac{h_y^2}{12}, & q = 0, \end{cases} \tag{15}$$

where h_y is the mesh size in y-direction.

When applied to the fourth order compact difference operators $L_x^{-1}A_x$ and $L_y^{-1}A_y$ to the steady 2D convection–diffusion equation in (4), it yields the following exponential fourth-order compact approximation:

$$(L_x^{-1}A_x + L_y^{-1}A_y)u_{ij} = f_{ij} + \mathrm{O}(h^4), \tag{16}$$

where $\mathrm{O}(h^4)$ denotes the $\mathrm{O}(h_x^4) + \mathrm{O}(h_y^4)$ term and (i, j) stands for the spatial position of (x_i, y_j).

By using (16), we can derive the exponential fourth-order ADI scheme for unsteady 2D convection–diffusion problem (1). Replacing f by $-\partial u/\partial t$, Eq. (16) may be written as

$$\left(\frac{\partial u^n}{\partial t}\right)_{ij} = -(L_x^{-1}A_x + L_y^{-1}A_y)u_{ij}^n + \mathrm{O}(h^4) \tag{17}$$

in which u^n is the approximate solution at time level $t^n = n\triangle t$, n represents the temporal level, and $\triangle t = t^{n+1} - t^n$ is the time step size. Eq. (17) is a fourth-order semi-discrete approximation to the unsteady convection–diffusion problem in (1). This semi-discrete approximation technique was also used in [13]. In the following u^n will be written in short for u_{ij}^n if there is no confusion about the notations. From the forward Taylor series development, we have

$$u^{n+1} = \left(1 + \Delta t\frac{\partial}{\partial t} + \frac{1}{2!}\Delta t^2\frac{\partial^2}{\partial t^2} + \frac{1}{3!}\Delta t^3\frac{\partial^3}{\partial t^3} + \cdots\right)u^n = \exp\left(\Delta t\frac{\partial}{\partial t}\right)u^n. \tag{18}$$

Applying (18) to (17), a fourth-order difference approximation of Eq. (1) is given by

$$u^{n+1} = \exp(-\Delta t\,(L_x^{-1}A_x + L_y^{-1}A_y))u^n, \tag{19}$$

$$\exp\left(\frac{\Delta t}{2}(L_x^{-1}A_x + L_y^{-1}A_y)\right)u^{n+1} = \exp\left(-\frac{\Delta t}{2}(L_x^{-1}A_x + L_y^{-1}A_y)\right)u^n. \tag{20}$$

Exploiting the commutativity of the difference operators A_x, A_y, L_x and L_y, which is possible since the convective and diffusive terms are assumed constant, yields

$$\exp\left(\frac{\Delta t}{2}L_x^{-1}A_x\right)\exp\left(\frac{\Delta t}{2}L_y^{-1}A_y\right)u^{n+1} = \exp\left(-\frac{\Delta t}{2}L_x^{-1}A_x\right)\exp\left(-\frac{\Delta t}{2}L_y^{-1}A_y\right)u^n, \tag{21}$$

using the Taylor expansions, it becomes

$$\begin{aligned}&\left(1 + \frac{\Delta t}{2}L_x^{-1}A_x\right)\left(1 + \frac{\Delta t}{2}L_y^{-1}A_y\right)u^{n+1} \\ &\quad = \left(1 - \frac{\Delta t}{2}L_x^{-1}A_x\right)\left(1 - \frac{\Delta t}{2}L_y^{-1}A_y\right)u^n + \mathrm{O}(\Delta t^3) + \mathrm{O}(\Delta t h^4),\end{aligned} \tag{22}$$

which is the Crank–Nicolson (C–N) time discretization if $\mathrm{O}(\Delta t^3) + \mathrm{O}(\Delta t h^4)$ is dropped. When applied to both sides of Eq. (22) with difference operator L_xL_y, we obtain

$$\left(L_x + \frac{\Delta t}{2}A_x\right)\left(L_y + \frac{\Delta t}{2}A_y\right)u^{n+1} = \left(L_x - \frac{\Delta t}{2}A_x\right)\left(L_y - \frac{\Delta t}{2}A_y\right)u^n + \mathrm{O}(\Delta t^3) + \mathrm{O}(\Delta t h^4). \tag{23}$$

To achieve unconditional stability, one may resort to a fully implicit or Crank–Nicolson method for time discretization of Eq. (17). This will result in a system of algebraic equations that is sparse, which may require a large amount of computational effort. One remedy is to use ADI methods, which only require solving one-dimensional implicit problems for each time step. The details of the ADI methods can be found in [27].

Now we introduce an exponential higher-order ADI scheme and the corresponding boundary conditions which will be used in our numerical solutions for the unsteady 2D convection–diffusion problems.

The resulting approximation (23) is second-order accurate in time and fourth-order accurate in space. From formula (23), we can obtain the following exponential high order ADI scheme. Introducing an intermediate variable u^*, Eq. (23) can be solved in two steps as

$$\left(L_x + \frac{\Delta t}{2}A_x\right)u^* = \left(L_x - \frac{\Delta t}{2}A_x\right)\left(L_y - \frac{\Delta t}{2}A_y\right)u^n, \tag{24a}$$

$$\left(L_y + \frac{\Delta t}{2}A_y\right)u^{n+1} = u^*. \tag{24b}$$

It is clear that Eq. (24) is the same as formula (23) within the accuracy $O(\Delta t^3) + (\Delta t h^4)$. Referring to Appendix A, we see that the resulting EHOC ADI scheme (24) in each ADI solution step give rise to a strictly diagonally dominant tridiagonal matrix which can be inverted by simple tridiagonal Gaussian decomposition, and, therefore, may be solved by application of the one-dimensional tridiagonal Thomas algorithm with a considerable saving in computing time.

The approximate solution u^n must satisfy the initial and boundary conditions (2) and (3), i.e.,

(i) $u^0 = u_0$, at all mesh points,
(ii) $u^n = g^n$, $n = 0, 1, \ldots, N$, on the boundary $\partial\Omega$.

The intermediate variable u^* introduced in each ADI scheme above is not necessarily an approximation to the solution at any time levels. The following formulae give u^* explicitly in terms of the central difference of g^{n+1} with respect to y from Eq. (3):

$$u^* = \left(L_y + \frac{\Delta t}{2}A_y\right)g^{n+1}. \tag{25}$$

If the boundary conditions are independent of the time, the formulae giving u^* on the boundary $\partial\Omega$ reduce to

$$u^* = \left(L_y + \frac{\Delta t}{2}A_y\right)g. \tag{26}$$

For the unsteady 2D convection diffusion equation with source term, we have the following high order ADI scheme:

$$\left(L_x + \frac{\Delta t}{2}A_x\right)u^* = \left(L_x - \frac{\Delta t}{2}A_x\right)\left(L_y - \frac{\Delta t}{2}A_y\right)u^n + \frac{\Delta t}{2}L_xL_y(S^{n+1} + S^n), \tag{27a}$$

$$\left(L_y + \frac{\Delta t}{2}A_y\right)u^{n+1} = u^*, \tag{27b}$$

or

$$\left(L_x + \frac{\Delta t}{2}A_x\right)u^* = \left(L_x - \frac{\Delta t}{2}A_x\right)\left(L_y - \frac{\Delta t}{2}A_y\right)u^n + \Delta t L_xL_yS^{n+1/2}, \tag{28a}$$

$$\left(L_y + \frac{\Delta t}{2}A_y\right)u^{n+1} = u^*, \tag{28b}$$

where $S^n = S(x_i, y_j, t_n)$, $S^{n+1/2} = S(x_i, y_j, t_n + \Delta t/2)$ and $S^n = S(x_i, y_j, t_{n+1})$. Eq. (27) or Eq. (28) is second-order accurate in time and fourth-order accurate in space.

3. Stability analysis

Following the von Neumann method for linear stability analysis, we assume that the numerical solution can be expressed by means of a Fourier series, whose typical term is

$$u_{ij}^n = \eta^n \exp\{I\theta_x i\} \exp\{I\theta_y j\}, \tag{29}$$

where $I = \sqrt{-1}$, η^n is the amplitude at time level n, and $\theta_x (= k_x h_x)$ and $\theta_y (= k_y h_y)$ are phase angles with the wavenumbers k_x and k_y in the x- and y-directions, respectively. Substituting the discrete Fourier mode (29) into (23), the amplification factor $G(\theta_x, \theta_y) = \eta^{n+1}/\eta^n$ can be written as

$$|G(\theta_x, \theta_y)| = |l(\theta_x)||l(\theta_y)|,$$

where $l(\theta_x)$ is given by

$$l(\theta_x) = \frac{(\gamma_1 - \gamma_2) + I(\gamma_3 - \gamma_4)}{(\gamma_1 + \gamma_2) + I(\gamma_3 + \gamma_4)} \tag{30}$$

with

$$\gamma_1 = 1 - \frac{4\alpha_2}{h_x^2}\sin^2\frac{\theta_x}{2}, \quad \gamma_2 = \frac{2\alpha\Delta t}{h_x^2}\sin^2\frac{\theta_x}{2}, \quad \gamma_3 = \frac{\alpha_1}{h_x}\sin\theta_x, \quad \gamma_4 = \frac{p\Delta t}{2h_x}\sin\theta_x$$

and the similar expression for $l(\theta_y)$ may be written by replacing θ_x by θ_y, h_x by h_y and p by q, and α, α_1 and α_2 by β, β_1 and β_2, respectively.

For stability it is sufficient that $|l(\theta_x)|^2 \leqslant 1$ and $|l(\theta_y)|^2 \leqslant 1$. Imposing this condition directly on (30) yields, $\gamma_1\gamma_2 + \gamma_3\gamma_4 \geqslant 0$ as a necessary and sufficient condition for $|l(\theta_x)|^2 \leqslant 1$. Direct calculation of $\gamma_1\gamma_2 + \gamma_3\gamma_4 \geqslant 0$ shows that

$$\begin{aligned}\gamma_1\gamma_2 + \gamma_3\gamma_4 &= \frac{2\alpha\Delta t}{h_x^2}\left(1 - \frac{4\alpha_2}{h_x^2}\sin^2\frac{\theta_x}{2}\right)\sin^2\frac{\theta_x}{2} + \frac{p\alpha_1\Delta t}{2h_x^2}\sin^2\theta_x \\ &= \frac{2\alpha\Delta t}{h_x^2}\left(1 - \frac{4\alpha_2}{h_x^2}\sin^2\frac{\theta_x}{2}\right)\sin^2\frac{\theta_x}{2} + \frac{2p\alpha_1\Delta t}{h_x^2}\left(1 - \sin^2\frac{\theta_x}{2}\right)\sin^2\frac{\theta_x}{2}.\end{aligned} \tag{31}$$

We will verify that $\gamma_1\gamma_2 + \gamma_3\gamma_4 \geqslant 0$. First assume that $p = 0$, then

$$\alpha = a, \quad \alpha_1 = 0, \quad \alpha_2 = \frac{h_x^2}{12}. \tag{32}$$

Substituting (32) into (31), gives

$$\gamma_1\gamma_2 + \gamma_3\gamma_4 = \frac{2a\Delta t}{h_x^2}\left(1 - \frac{1}{3}\sin^2\frac{\theta_x}{2}\right)\sin^2\frac{\theta_x}{2}. \tag{33}$$

Since $a > 0$ and $0 \leqslant \sin^2\theta_x/2 \leqslant 1$, we conclude that $\gamma_1\gamma_2 + \gamma_3\gamma_4 \geqslant 0$ for all $\theta_x \in [-\pi, \pi]$. Assume now that $p \neq 0$, then

$$\alpha_1 = \frac{a - \alpha}{p}, \quad \alpha_2 = \frac{a(a - \alpha)}{p^2} + \frac{h_x^2}{6}. \tag{34}$$

Substituting (34) into (31) we have

$$\begin{aligned}\gamma_1\gamma_2 + \gamma_3\gamma_4 &= \frac{2\Delta t}{h_x^2}\left[\alpha\left(1 - \frac{4\alpha_2}{h_x^2}\right)\sin^2\frac{\theta_x}{2} + a\left(1 - \sin^2\frac{\theta_x}{2}\right)\right]\sin^2\frac{\theta_x}{2} \\ &= \frac{2\Delta t}{h_x^2}\left\{\alpha\left[\left(\frac{1}{3} - \frac{4a(a - \alpha)}{p^2h_x^2}\right)\right]\sin^2\frac{\theta_x}{2} + a\left(1 - \sin^2\frac{\theta_x}{2}\right)\right\}\sin^2\frac{\theta_x}{2}.\end{aligned} \tag{35}$$

Given that $x\coth(x) > 0$ for all real x (except at $x = 0$) and $a > 0$, we have

$$\alpha = \frac{ph_x}{2}\coth\left(\frac{ph_x}{2a}\right) = a\frac{ph_x}{2a}\coth\left(\frac{ph_x}{2a}\right) > 0. \tag{36}$$

Since $1 - x\coth(x) < 0$ for all non-zero real x (see, Proposition 3 in Appendix B), we find that $a - \alpha = a[1 - ph_x/2a\coth(ph_x/2a)] < 0$ and hence

$$\frac{1}{3} - \frac{4a(a-\alpha)}{p^2h_x^2} > 0. \tag{37}$$

Since $0 \leqslant \sin^2\theta_x/2 \leqslant 1$, the following inequality holds by virtue of (36) and (37):

$$\alpha\left[\left(\frac{1}{3} - \frac{4a(a-\alpha)}{p^2h_x^2}\right)\right]\sin^2\frac{\theta_x}{2} + a\left(1 - \sin^2\frac{\theta_x}{2}\right) > 0. \tag{38}$$

As a result,

$$\gamma_1\gamma_2 + \gamma_3\gamma_4 = \frac{2\Delta t}{h_x^2}\left\{\alpha\left[\left(\frac{1}{3} - \frac{4a(a-\alpha)}{p^2h_x^2}\right)\right]\sin^2\frac{\theta_x}{2} + a\left(1 - \sin^2\frac{\theta_x}{2}\right)\right\}\sin^2\frac{\theta_x}{2} \geqslant 0. \tag{39}$$

Hence, $\gamma_1\gamma_2 + \gamma_3\gamma_4 \geqslant 0$, and it follows that $|l(\theta_x)|^2 \leqslant 1$. In the same way, we may find that $|l(\theta_y)|^2 \leqslant 1$. Thus the proposed method when applied to the unsteady 2D linear convection–diffusion equation is unconditionally stable.

4. Numerical experiments

In this section, we perform numerical experiments to illustrate the validity and effectiveness of the proposed exponential higher order compact ADI (EHOC ADI) method. The numerical results of three test problems possessing exact solution are given. For these problems we will compare with the numerical results of major methods involving the Karaa and Zhang ADI (HOC ADI) scheme [13], the Peaceman–Rachford ADI (P–R ADI) scheme [19], the fourth-order nine-point compact implicit scheme [12] and the spatial third-order nine-point compact implicit scheme [17]. The ADI methods used were performed by repeatedly solving a series of triangular linear systems, while to solve the linear system arising from the Noye and Tan difference discretization and the Kalita et al. difference discretization, we used a line Gauss–Seidel iteration. The iteration process was repeated until the 2-norm of the relative residual was reduced to 10^{-10}. All results were run on a SONY PCG-V505MCP computer using double precision arithmetic.

4.1. Problem 1

Consider a pure diffusion equation in the unit square domain $0 \leqslant x, y \leqslant 1$ with diffusion coefficients $a = b = 1$ (and $p = q = 0$). The analytical solution to this equation is given by

$$u(x, y, t) = \mathrm{e}^{-2\pi^2 t}\sin(\pi x)\sin(\pi y). \tag{40}$$

The Dirichlet boundary and initial conditions are directly taken from this analytical solution. The numerical solutions, using the present EHOC ADI scheme and the P–R ADI scheme [19], are obtained under uniform grids ($h = h_x = h_y$) with different mesh sizes and compared their accuracy under the L^2 norm error of the numerical solution with respect to the analytical solution. The comparison of numerical results are given in Tables 1 and 2. Note that the approximation solution from the present ADI method is more accurate than that from the P–R ADI method. In Table 1, we choose $\Delta t = h^2$ and $t = 0.125$ for the verifications of fourth-order accuracy in space and second-order accuracy in time. The rate of convergence is estimated by using the $\ln_2(err1/err2)$, where $err1$ and $err2$ are L^2 norm errors with the grid sizes h and $h/2$, respectively. These values are approximately 4 and 2 for the present ADI method and the P–R ADI method, respectively. Notice also that L^2 norm errors on 11×11 grid nodes are almost the same as those using the P–R ADI scheme on 41×41 grid nodes. Table 2 depicts, at $h = 1/10$ and $t = 0.25$, L^2 norm errors with various time steps for different schemes. In this case, the results of the present ADI method become more and more accurate with the reduction in time step, while the ones of the P–R ADI method are almost invariable. The results in Tables 1 and 2 show the superiority of the EHOC ADI scheme over the P–R ADI scheme.

Table 1
L^2 norm errors and the convergence rate with $\Delta t = h^2$, $t = 0.125$

Grid	P–R ADI method		Present ADI method	
	L^2 norm error	Rate	L^2 norm error	Rate
$11 \cdot 11$	$8.28094 \cdot 10^{-4}$	—	$8.55134 \cdot 10^{-5}$	—
$21 \cdot 21$	$2.16396 \cdot 10^{-4}$	1.936	$5.19160 \cdot 10^{-6}$	4.041
$41 \cdot 41$	$5.38654 \cdot 10^{-5}$	2.006	$3.17475 \cdot 10^{-7}$	4.031

Table 2
L^2 norm errors at $h_x = h_y = 0.1$, $t = 0.25$ with different time steps

Δt	P–R ADI method	Present ADI method
	L^2 norm error	L^2 norm error
0.0125	$1.52587 \cdot 10^{-4}$	$2.64692 \cdot 10^{-5}$
0.00625	$1.57365 \cdot 10^{-4}$	$5.40813 \cdot 10^{-6}$
0.003125	$1.54384 \cdot 10^{-4}$	$7.18040 \cdot 10^{-7}$

Table 3
Errors at $t = 1.25$ and CPU times of five FDMs, with $\Delta t = 0.00625$ and $h_x = h_y = 0.025$, *Problem 2*

Method	Average error	L^∞ norm error	L^2 norm error	CPU time (s)
Noye and Tan	$1.971 \cdot 10^{-5}$	$6.509 \cdot 10^{-4}$	$1.280 \cdot 10^{-4}$	25.19
Kalita et al.	$1.597 \cdot 10^{-5}$	$4.477 \cdot 10^{-4}$	$1.024 \cdot 10^{-4}$	9.20
P–R ADI	$3.109 \cdot 10^{-4}$	$7.778 \cdot 10^{-3}$	$2.025 \cdot 10^{-3}$	1.02
Karaa and Zhang ADI	$9.218 \cdot 10^{-6}$	$2.500 \cdot 10^{-4}$	$5.931 \cdot 10^{-5}$	1.06
Present ADI	$9.663 \cdot 10^{-6}$	$2.664 \cdot 10^{-4}$	$6.194 \cdot 10^{-5}$	1.08

4.2. Problem 2

Consider now a special problem in the square domain $0 \leqslant x, y \leqslant 2$, with an analytical solution given, as in [17], by

$$u(x, y, t) = \frac{1}{4t+1} \exp\left[-\frac{(x - pt - 0.5)^2}{a(4t+1)} - \frac{(y - qt - 0.5)^2}{b(4t+1)} \right]. \tag{41}$$

The Dirichlet boundary and initial conditions are directly taken from this analytical solution. For the sake of comparison, we choose $a = b = 0.01$ and $p = q = 0.8$.

The average errors, the L^∞ norms errors, the L^2 norms errors and the CPU time used, using the Karaa and Zhang ADI (HOC ADI) scheme [13], the P–R ADI scheme [19], the implicit fourth-order nine-point compact scheme [12], the spatial third-order nine-point compact scheme [17] and the present ADI (EHOC ADI) scheme, are given in Table 3. The errors of the HOC ADI method and the EHOC ADI method are almost identical and they provide the most accurate solution as seen from Table 3. A remarkably similar picture (Fig. 1(b)) is obtained from the analytical solution (Fig. 1(a)) where at $t = 1.25$ the Gaussian pulse moves to a position centered at (1.5,1.5) with a pulse height of 1/6. A comparison of Fig. 1(a) and (c) shows that the P–R ADI scheme is not accurate to capture the original pulse and the pulse distribution is distorted slightly. This fact can be seen by observing the position of grid lines and contour plots of solution surface in Fig. 1 and is also reflected in Fig. 2(b). Fig. 3 contain contour curves for the analytical and computed pulses in the sub-region $1 \leqslant x, y \leqslant 2$ for each test carried out. An analysis of pictures shows that the present EHOC ADI scheme, the HOC ADI scheme [13] and the Kalita et al. scheme [12] as well as the Noye and Tan [17] capture very well the moving pulse, yielding pulses centered at (1.5, 1.5) and almost indistinguishable from the exact one. From Figs. 1(c), 2(b) and 3(f), however, we note that the P–R ADI scheme produces a pulse distorted in both the

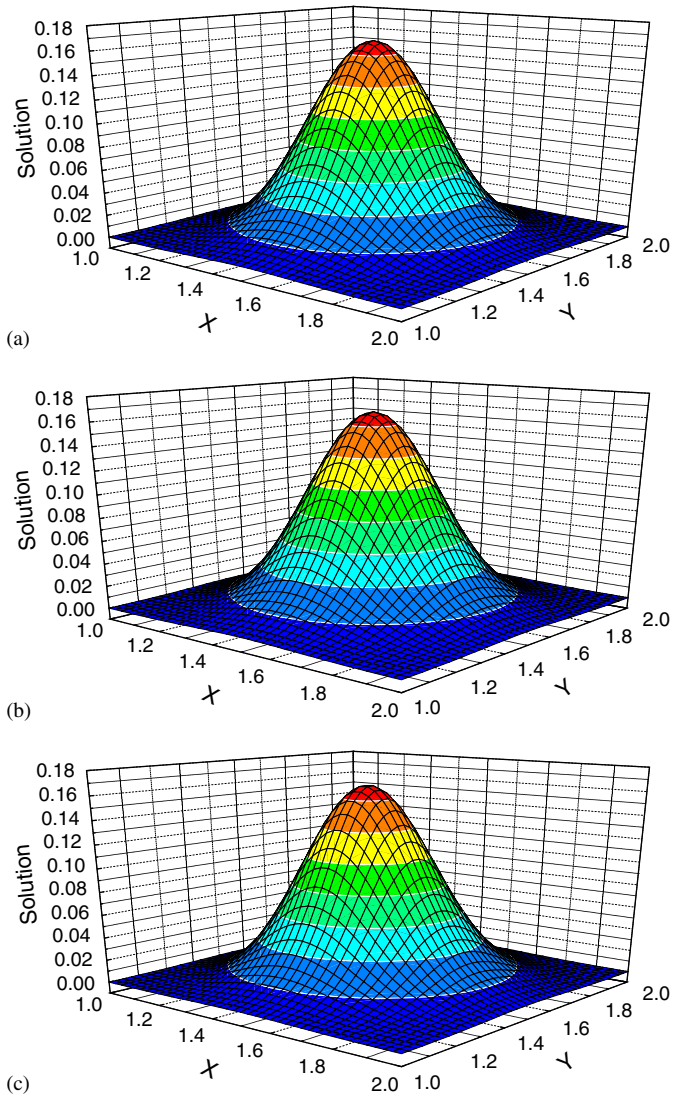

Fig. 1. Solution surface plots of exact (a), numerical [$\Delta t = 0.0625$] (b) (present ADI scheme) and (c) (P–R ADI scheme) pulse in the sub-region $1 \leqslant x, y \leqslant 2$ at $t = 1.25$ s.

x- and y-direction. As is explained in [17], this is due to the fact the second-order error terms of method is related to the wave numbers in both directions. We also notice that the three ADI methods exhibit very small CPU times from Table 3. The CPU time ratio of the EHOC ADI method or the HOC ADI method [13] to the Noye and Tan method is approximately 25.0. This clearly shows, for Problem 2, the present EHOC ADI method and the HOC ADI method are the most effective in terms of accuracy and time consumption.

4.3. Problem 3

Consider a two-dimensional steady-state convection diffusion equation in the unit square domain $0 \leqslant x, y \leqslant 1$ with diffusion coefficients $a = b = 1$ and convection coefficients $p = -2Re$, $q = 2Re$. The analytical solution to this equation is given by

$$u(x, y) = \frac{e^{2Re(1-x)} + e^{2Rey} - 2}{e^{2Re} - 1}. \tag{42}$$

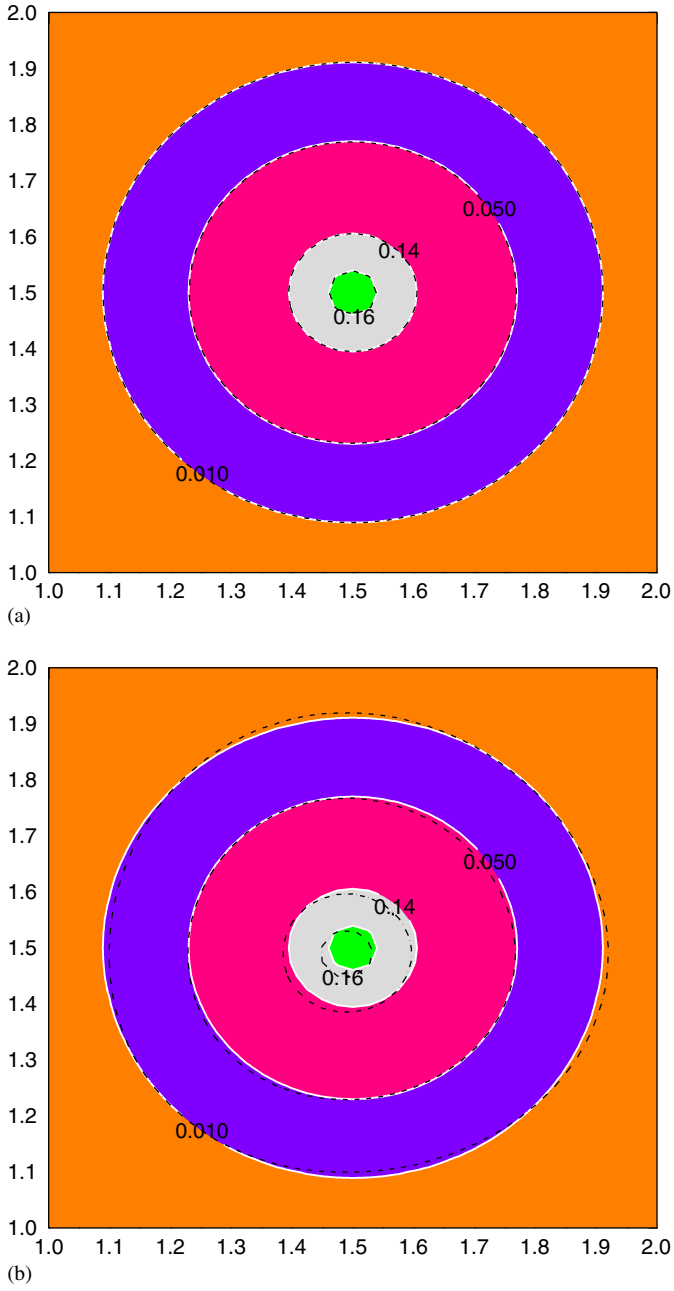

Fig. 2. Contour lines (0.16, 0.14, 0.05 and 0.01) of the pulse in the sub-region $1 \leqslant x, y \leqslant 2$ at $t = 1.25$ s: (a) exact (white solid) and the present ADI scheme (black dash dot) and (b) exact (white solid) and the P–R ADI scheme (black dash dot) [$\Delta t = 0.0625$].

The Dirichlet boundary conditions are directly taken from this analytical solution. This problem, which was used as a test one in [30], has steep boundary layers near $x = 0$ and $y = 1$, Computations, using the present EHOC ADI scheme and the HOC ADI scheme [13], are carried out on uniform grids of sizes 65×65 with a time step $\Delta t = 0.01$ for $1 \leqslant Re \leqslant 10^5$. For comparison purposes, the model equation is also solved with the Kalita et al. scheme [12] and the Noye and Tan scheme [17] with a time step $\Delta t = 0.001$ for $1 \leqslant Re \leqslant 10^5$. Initial guess was zero. The iteration process

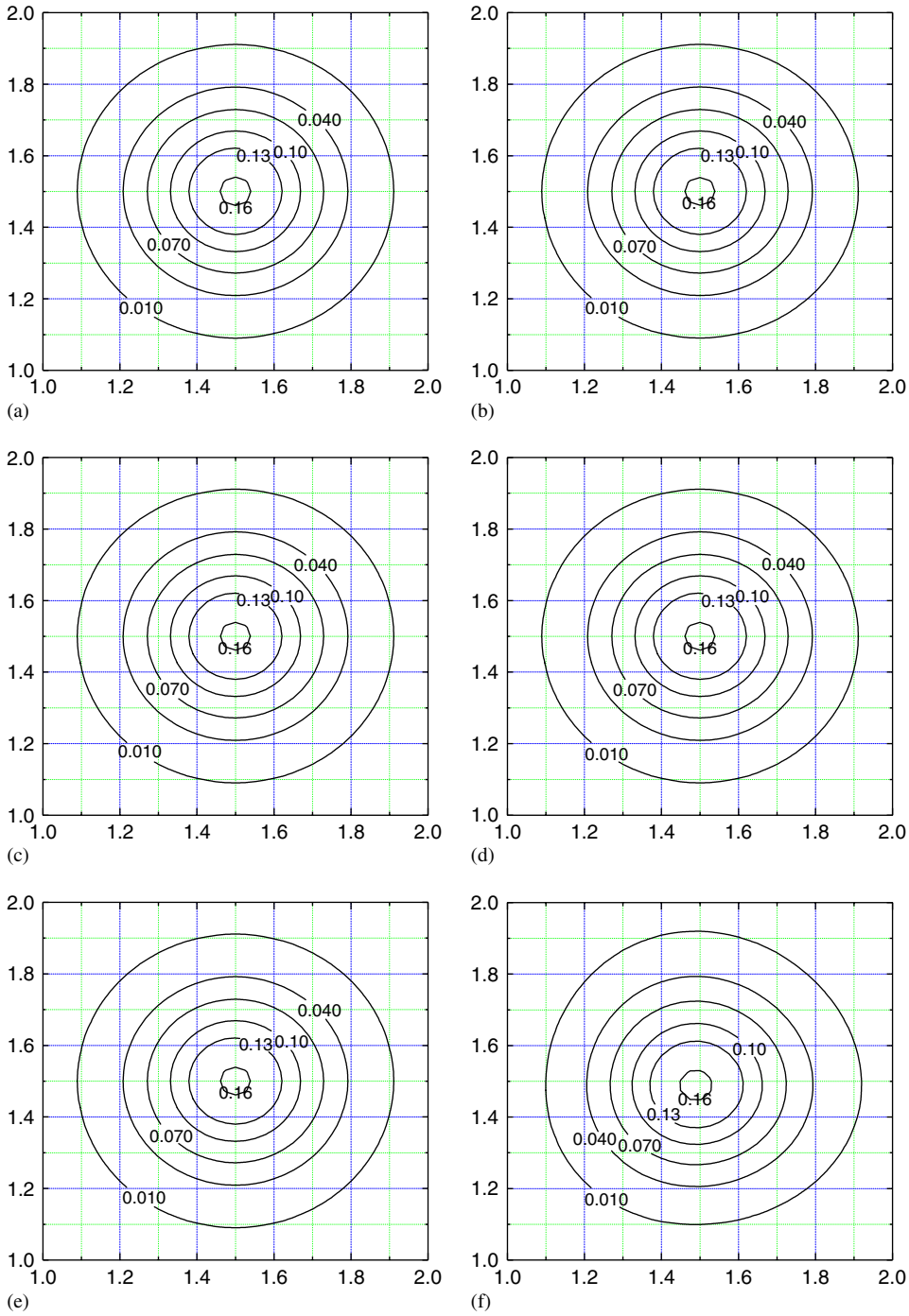

Fig. 3. Contour lines of the pulse in the sub-region $1 \leqslant x, y \leqslant 2$ at $t = 1.25$ s: (a) exact, (b) present ADI scheme, (c) Noye and Tan scheme, (d) Kalita et al. scheme, (e) Karaa and Zhang ADI scheme, and (f) P–R ADI scheme, with $\Delta t = 0.0625$.

was repeated until

$$|u^{(k+1)} - u^{(k)}| \leqslant 10^{-14}$$

Table 4
Errors and CPU times of two high-order ADI methods, with $\Delta t = 0.01$ and $h_x = h_y = 1/64$, *Problem 3*

Re	Karaa and Zhang ADI method			Present ADI method		
	L^∞ norm error	L^2 norm error	CPU time (s)	L^∞ norm error	L^2 norm error	CPU time (s)
1	$3.58 \cdot 10^{-10}$	$1.91 \cdot 10^{-10}$	5.55	$2.61 \cdot 10^{-13}$	$1.81 \cdot 10^{-14}$	5.21
10	$8.07 \cdot 10^{-6}$	$2.00 \cdot 10^{-6}$	1.34	$3.94 \cdot 10^{-14}$	$6.82 \cdot 10^{-15}$	1.27
10^2	$5.70 \cdot 10^{-2}$	$5.38 \cdot 10^{-3}$	0.37	$3.03 \cdot 10^{-15}$	$2.16 \cdot 10^{-16}$	0.35
10^3	$6.82 \cdot 10^{-1}$	$1.61 \cdot 10^{-1}$	0.68	$2.41 \cdot 10^{-15}$	$2.13 \cdot 10^{-16}$	0.08
10^4	$8.74 \cdot 10^{-1}$	$4.58 \cdot 10^{-1}$	3.02	$3.39 \cdot 10^{-17}$	$1.94 \cdot 10^{-18}$	0.08
10^5	$7.47 \cdot 10^{-1}$	$4.03 \cdot 10^{-1}$	26.45	$2.14 \cdot 10^{-17}$	$1.44 \cdot 10^{-18}$	0.07

Table 5
Errors and CPU times of two 9-point compact methods, with $\Delta t = 0.001$ and $h_x = h_y = 1/64$, *Problem 3*

Re	Kalita et al. method			Noye and Tan method		
	L^∞ norm error	L^2 norm error	CPU time (s)	L^∞ norm error	L^2 norm error	CPU time (s)
1	$3.58 \cdot 10^{-10}$	$1.91 \cdot 10^{-10}$	52.81	$2.20 \cdot 10^{-5}$	$1.18 \cdot 10^{-5}$	49.45
10	$8.07 \cdot 10^{-6}$	$2.00 \cdot 10^{-6}$	28.90	$5.00 \cdot 10^{-3}$	$1.23 \cdot 10^{-3}$	29.70
10^2	$5.70 \cdot 10^{-2}$	$5.38 \cdot 10^{-3}$	97.47	$6.49 \cdot 10^{-1}$	$4.71 \cdot 10^{-2}$	8.95
10^3	div.	div.	n.r.	2.89	$3.29 \cdot 10^{-1}$	178.43
10^4	div.	div.	n.r.	div.	div.	n.r.
10^5	div.	div.	n.r.	div.	div.	n.r.

Note: div. = divergence, n.r. = no result.

for all grid points, where k is the iterative count. The L^∞ norms errors and L^2 norms errors of the computed solution with respect to the analytical solution and the CPU times used are listed in Tables 4 and 5. It is shown that (i) for small *Re* the present EHOC ADI scheme can give much more accurate results than the HOC ADI scheme [13], the Kalita et al. scheme [12] and the Noye and Tan scheme [17], although the CPU times of the HOC ADI method and the EHOC ADI method are identical; (ii) for convection-dominated cases with large *Re*, the present EHOC ADI scheme can resolve accurately the boundary layer, the HOC ADI scheme [13] givers only very poor results, and uses much more CPU times than the present EHOC ADI scheme, while the Kalita et al. scheme [12] and the Noye and Tan scheme [17] are divergence. Numerical solutions computed by the present ADI method and the Karaa and Zhang ADI method for $Re = 1$, 1000 and 100,000 are also presented in Fig. 4. It is seen from the figure that both methods produce acceptable solutions for $Re = 1$, being nearly nodally exact. The HOC ADI method solutions are inacceptable for convection-dominated cases with $Re = 1000, 100, 000$. In contrast, the EHOC ADI method yields nodally accurate monotone solutions, demonstrating the ability to resolve sharp gradients in a boundary layer.

5. Conclusion and remarks

We have established an exponential high-order compact alternating direction implicit method for the numerical solution of unsteady 2D convection–diffusion problems. The method is second-order in time and fourth-order in space and only involves three-point stencil for each one-dimensional operator. The unconditionally stable character of the proposed EHOC ADI difference scheme have been verified by a discrete Fourier analysis. A distinguishing desirable property of the developed method is solution matrix bandwidth, which always remains equal to that of the second-order discretizations. The resulting EHOC ADI scheme in each ADI solution step corresponds to a strictly diagonally dominant tridiagonal matrix equation which can be inverted by simple tridiagonal Gaussian decomposition and may be solved by application of the one-dimensional tridiagonal Thomas algorithm with a considerable saving in computing time. This permits combining the computational efficiency of the lower order methods with superior accuracy inherent

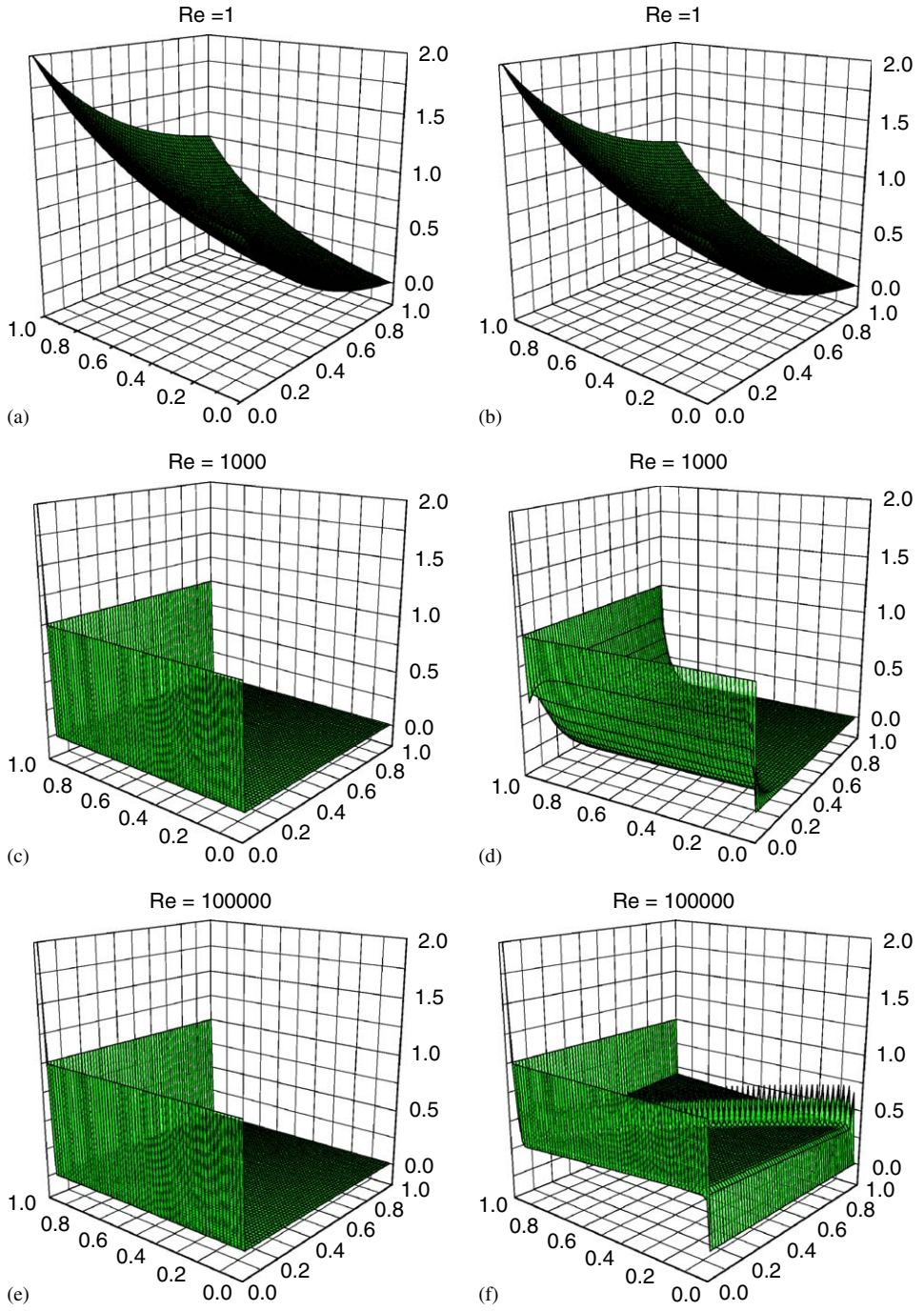

Fig. 4. Solutions of Problem 3 with $Re = 1$, $Re = 1000$ and $Re = 100,000$on a 64×64 square mesh: (a), (c) and (e) the EHOC ADI method; (b), (d) and (f) the HOC ADI method.

in high order approximations. The present method is easily extendible to multi-dimensional problems.

Numerical experiments are performed to demonstrate its high accuracy and efficiency and to show its superiority over the spatial nine-point third-order compact scheme of Noye and Tan, the fourth-order nine-point compact scheme of Kalita et al., the polynomial HOC ADI method and the classical Peaceman–Rachford ADI scheme, in terms of accuracy

and/or computational cost. The robustness of the present method is illustrated by its applicability to one steady and two unsteady problems. The computational results show the present EHOC ADI method successfully combined accuracy, efficiency and robustness and required significantly fewer number of grid nodes to accurately resolve solution gradients for the convection-dominated problem. The present ADI method is applicable to other problems with temporally and/or spatially dependent coefficients. A fourth-order ADI method for the unsteady 2D convection diffusion equation with variable convention coefficients is presently being examined and results would be presented in future. We are currently working to extend the present EHOC ADI method to fluid flow problems for larger values of Reynolds numbers.

Acknowledgements

This work was supported in part by the Teaching and Research Award Program for Outstanding Young Teachers in Higher Education Institutions of MOE, China, the National Natural Science Foundation of China under Grant 19702008, Science Foundation of Higher Education Institutions in Ningxia, China and the High Performance Computing Foundation of China under Grant 99107 and 00108.

Appendix A. Proof of the strictly diagonal dominance

This appendix is devoted to a detailed proof that the tridiagonal systems of equations produced by schemes (24) are strictly diagonally dominant. Under this condition, the resulting tridiagonal system of equations has a unique solution. Since the left-hand sides of the (24a) and (24b) is just the same in the form, we consider only (24b) without loss of generality. Using the scheme derived in Section 3, we can write the discretization equation for Eq. (24b) as

$$A_{i,j}u_{i,j-1} + B_{i,j}u_{i,j} + C_{i,j}u_{i,j+1} = u^*_{i,j}, \tag{A.1}$$

it results a linear system with the coefficient matrix

$$Q = \mathrm{tri}[A_{i,j}, B_{i,j}, C_{i,j}], \tag{A.2}$$

where

$$A_{i,j} = \frac{\beta_2}{h_y^2} - \frac{\beta_1}{2h_y} - \frac{\Delta t}{2}\left(\frac{\beta}{h_y^2} + \frac{q}{2h_y}\right), \tag{A.3}$$

$$B_{i,j} = 1 - \frac{2\beta_2}{h_y^2} + \frac{\Delta t\beta}{h_y^2}, \tag{A.4}$$

$$C_{i,j} = \frac{\beta_2}{h_y^2} + \frac{\beta_1}{2h_y} - \frac{\Delta t}{2}\left(\frac{\beta}{h_y^2} - \frac{q}{2h_y}\right). \tag{A.5}$$

Note that if $|B_{i,j}| > |A_{i,j}| + |C_{i,j}|$ hold, it follows that the matrix Q is diagonally dominant. It is easily found that $|1-\frac{2\beta_2}{h_y^2}|+|\frac{\Delta t\beta}{h_y^2}| > |\frac{\beta_2}{h_y^2}-\frac{\beta_1}{2h_y}|+|\frac{\beta_2}{h_y^2}+\frac{\beta_1}{2h_y}|+|\frac{\Delta t}{2}(\frac{\beta}{h_y^2}+\frac{q}{2h_y})|+|\frac{\Delta t}{2}(\frac{\beta}{h_y^2}-\frac{q}{2h_y})|$ is a sufficient condition for $|B_{i,j}| > |A_{i,j}|+|C_{i,j}|$. Direct calculation show that

$$\left|-\frac{\beta}{h_y^2} - \frac{q}{2h_y}\right| = \left|\frac{-qe^x}{h_y(e^x - e^{-x})}\right| = \frac{qe^x}{h_y(e^x - e^{-x})} = \frac{\beta}{h_y^2} + \frac{q}{2h_y}, \tag{A.6}$$

$$\left|-\frac{\beta}{h_y^2} + \frac{q}{2h_y}\right| = \left|\frac{-qe^{-x}}{h_y(e^x - e^{-x})}\right| = \frac{qe^{-x}}{h_y(e^x - e^{-x})} = \frac{\beta}{h_y^2} - \frac{q}{2h_y}, \tag{A.7}$$

$$\left|\frac{2\beta}{h_y^2}\right| = \left|\frac{q(e^x + e^{-x})}{h_y(e^x - e^{-x})}\right| = \frac{q(e^x + e^{-x})}{h_y(e^x - e^{-x})} = \frac{2\beta}{h_y^2}, \tag{A.8}$$

where in this appendix context $x = qh_y/2b$. It follows form (A.6), (A.7) and (A.8) that

$$\left|\frac{\Delta t\beta}{h_y^2}\right| = \left|-\frac{\Delta t}{2}\left(\frac{\beta}{h_y^2}+\frac{q}{2h_y}\right)\right| + \left|-\frac{\Delta t}{2}\left(\frac{\beta}{h_y^2}-\frac{q}{2h_y}\right)\right|. \tag{A.9}$$

Now we prove that

$$\left|1-\frac{2\beta_2}{h_y^2}\right| > \left|\frac{\beta_2}{h_y^2}-\frac{\beta_1}{2h_y}\right| + \left|\frac{\beta_2}{h_y^2}+\frac{\beta_1}{2h_y}\right|.$$

First, note that when $q = 0$,

$$\beta = b, \quad \beta_1 = 0, \quad \beta_2 = \frac{h_y^2}{12}, \tag{A.10}$$

thus, we have

$$1-\frac{2\beta_2}{h_y^2} = \frac{5}{6}, \quad \frac{\beta_2}{h_y^2}-\frac{\beta_1}{2h_y} = \frac{1}{12}, \quad \frac{\beta_2}{h_y^2}+\frac{\beta_1}{2h_y} = \frac{1}{12}. \tag{A.11}$$

Obviously, from the above results, gives

$$\left|1-\frac{2\beta_2}{h_y^2}\right| > \left|\frac{\beta_2}{h_y^2}-\frac{\beta_1}{2h_y}\right| + \left|\frac{\beta_2}{h_y^2}+\frac{\beta_1}{2h_y}\right|. \tag{A.12}$$

Notice also that when $q \neq 0$,

$$1-\frac{2\beta_2}{h_y^2} = 1-\frac{2}{h_y^2}\left(\frac{b(b-\beta)}{q^2}+\frac{h_y^2}{6}\right) = \frac{2}{3}-\frac{1-x\coth x}{2x^2}, \tag{A.13}$$

$$\frac{\beta_2}{h_y^2}+\frac{\beta_1}{2h_y} = \frac{1}{h_y^2}\left(\frac{b(b-\beta)}{q^2}+\frac{h_y^2}{6}\right)+\frac{b-\beta}{2qh_y} = \frac{1-x\coth x}{4x^2}+\frac{1}{6}+\frac{1-x\coth x}{4x}, \tag{A.14}$$

$$\frac{\beta_2}{h_y^2}-\frac{\beta_1}{2h_y} = \frac{1}{h_y^2}\left(\frac{b(b-\beta)}{q^2}+\frac{h_y^2}{6}\right)-\frac{b-\beta}{2qh_y} = \frac{1-x\coth x}{4x^2}+\frac{1}{6}-\frac{1-x\coth x}{4x}. \tag{A.15}$$

Since $1 - x\coth x < 0$ for all non-zero real x, we have

$$\frac{1-x\coth x}{x^2} < 0. \tag{A.16}$$

Referring Appendix B, we see that $-1 < \frac{1-x\coth x}{x} < 0$ if $x > 0$ and $0 < \frac{1-x\coth x}{x} < 1$ if $x < 0$ hold. When $x > 0$,

$$\left|\frac{1}{6}+\frac{1-x\coth x}{4x}\right| = \begin{cases} \dfrac{1}{6}+\dfrac{1-x\coth x}{4x}, & -\dfrac{4}{6} < \dfrac{1-x\coth x}{x} < 0, \\ \dfrac{x\coth x-1}{4x}-\dfrac{1}{6}, & -1 < \dfrac{1-x\coth x}{x} \leqslant -\dfrac{4}{6}, \end{cases} \tag{A.17}$$

$$\left|\frac{1}{6}-\frac{1-x\coth x}{4x}\right| = \frac{1}{6}-\frac{1-x\coth x}{4x}. \tag{A.18}$$

Adding (A.17) and (A.18), we obtain

$$\left|\frac{1}{6}+\frac{1-x\coth x}{4x}\right| + \left|\frac{1}{6}-\frac{1-x\coth x}{4x}\right| = \begin{cases} \dfrac{1}{3}, & -\dfrac{4}{6} < \dfrac{1-x\coth x}{x} < 0, \\ \dfrac{x\coth x-1}{2x}, & -1 < \dfrac{1-x\coth x}{x} \leqslant -\dfrac{4}{6}. \end{cases} \tag{A.19}$$

By (A.19) and since $-1 < \frac{1-x\coth x}{x} \leqslant 0$ in x for $x > 0$, we find at once

$$\left|\frac{1}{6}+\frac{1-x\coth x}{4x}\right|+\left|\frac{1}{6}-\frac{1-x\coth x}{4x}\right|<\frac{1}{2}. \tag{A.20}$$

Hence we obtain, by using the triangle inequality and (A.13), (A.16) and (A.20),

$$\begin{aligned}
&\left|\frac{\beta_2}{h_y^2}+\frac{\beta_1}{2h_y}\right|+\left|\frac{\beta_2}{h_y^2}-\frac{\beta_1}{2h_y}\right| \\
&\leqslant \left|\frac{1-x\coth x}{4x^2}+\frac{1}{6}+\frac{1-x\coth x}{4x}\right|+\left|\frac{1-x\coth x}{4x^2}+\frac{1}{6}-\frac{1-x\coth x}{4x}\right| \\
&\leqslant \left|\frac{1-x\coth x}{4x^2}\right|+\left|\frac{1}{6}+\frac{1-x\coth x}{4x}\right|+\left|\frac{1-x\coth x}{4x^2}\right|+\left|\frac{1}{6}-\frac{1-x\coth x}{4x}\right| \\
&= \frac{x\coth x-1}{2x^2}+\left|\frac{1}{6}+\frac{1-x\coth x}{4x}\right|+\left|\frac{1}{6}-\frac{1-x\coth x}{4x}\right| \\
&< \frac{x\coth x-1}{2x^2}+\frac{1}{2}<\frac{x\coth x-1}{2x^2}+\frac{2}{3} \\
&= \frac{2}{3}-\frac{1-x\coth x}{2x^2}=1-\frac{2\beta_2}{h_y^2} \\
&= \left|1-\frac{2\beta_2}{h_y^2}\right|.
\end{aligned} \tag{A.21}$$

The argument for $x < 0$ is analogous. Thus, we obtain that

$$\left|1-\frac{2\beta_2}{h_y^2}\right|>\left|\frac{\beta_2}{h_y^2}+\frac{\beta_1}{2h_y}\right|+\left|\frac{\beta_2}{h_y^2}-\frac{\beta_1}{2h_y}\right| \tag{A.22}$$

for all real x. Hence from (A.9) and (A.22),

$$\left|1-\frac{2\beta_2}{h_y^2}\right|+\left|\frac{\Delta t\beta}{h_y^2}\right|>\left|\frac{\beta_2}{h_y^2}-\frac{\beta_1}{2h_y}\right|+\left|\frac{\beta_2}{h_y^2}+\frac{\beta_1}{2h_y}\right|+\left|\frac{\Delta t}{2}\left(\frac{\beta}{h_y^2}+\frac{q}{2h_y}\right)\right|+\left|\frac{\Delta t}{2}\left(\frac{\beta}{h_y^2}-\frac{q}{2h_y}\right)\right|.$$

This completes the proof. □

Appendix B. Propositions and proof

This appendix is devoted to some propositions needed in the paper.

Proposition 1. $x-\cosh(x)\sinh(x)<0$, $x\in(0,+\infty)$.

Proof. Define a function $\phi(x)=x-\cosh(x)\sinh(x)$ on $[0,+\infty)$. Clearly, $\phi(x)$ is continuous and differentiable, and

$$\phi'(x)=-2\sinh^2(x),\quad x\in(0,+\infty).$$

Since $\phi'(x)=-2\sinh^2(x)<0$ in $(0,+\infty)$, $\phi(x)$ is strictly decreasing on $[0,+\infty)$. It follows from $\phi(0)=0$ that $\phi(x)<0$, i.e., $x-\cosh(x)\sinh(x)<0$ in $(0,+\infty)$. □

Proposition 2. $x^2-\sinh^2(x)<0$, $x\in(-\infty,0)\cup(0,+\infty)$.

Proof. Define a function $\chi(x)=x^2-\sinh^2(x)$ on $[0,+\infty)$. Clearly, $\chi(x)$ is continuous and differentiable, and

$$\chi'(x)=2[x-\cosh(x)\sinh(x)],\quad x\in(0,+\infty).$$

Since $x - \cosh(x)\sinh(x) < 0$ in $(0, +\infty)$ (see Proposition 1), we have $\chi'(x) < 0$ in $(0, +\infty)$ and it means that $\chi(x)$ is strictly decreasing on $[0, +\infty)$. Hence $\chi(x) < \chi(0)$, i.e., $x^2 - \sinh^2(x) < 0$ in $(0, +\infty)$. Finally, since $x^2 - \sinh^2(x)$ is even function on $(-\infty, +\infty)$, we conclude that $x^2 - \sinh^2(x) < 0$ in $(-\infty, 0) \cup (0, +\infty)$. □

Proposition 3. $1 - x\coth x < 0$, $x \in (-\infty, 0) \cup (0, +\infty)$.

Proof. Define a function $\varphi(x) = 1 - x\coth x$ on $[0, +\infty)$, where $\varphi(0) = \lim_{x\to 0}(1 - x\coth x) = 0$. It is easily seen that $\varphi(x)$ is continuous and differentiable. Taking the derivative,

$$\varphi'(x) = \frac{x - \sinh(x)\cosh(x)}{\sinh^2(x)}, \quad x \in (0, +\infty).$$

Using $x - \sinh(x)\cosh(x) < 0$ (see Proposition 1), we have $\varphi'(x) < 0$ in $(0, +\infty)$ and it implies that $\varphi(x)$ is strictly decreasing on $[0, +\infty)$. Hence $\varphi(x) < \varphi(0)$, i.e., $1 - x\coth x < 0$ in $(0, +\infty)$. Noting that $\varphi(-x) = \varphi(x)$, we conclude that $1 - x\coth x < 0$ for all non-zero real x. □

Proposition 4. (i) $-1 < \frac{1-x\coth x}{x} < 0$, $x \in (0, +\infty)$; (ii) $0 < \frac{1-x\coth x}{x} < 1$, $x \in (-\infty, 0)$.

Proof. (i) Define a function $\psi(x) = \frac{1-x\coth x}{x}$ on $[0, +\infty)$, where $\psi(0) = \lim_{x\to 0}\frac{1-x\coth x}{x} = 0$. Clearly, $\psi(x)$ is continuous on $[0, +\infty)$ and $\psi'(x) = \frac{x^2-\sinh^2 x}{x^2\sinh^2 x}$ in $(0, +\infty)$. Since $x^2 - \sinh^2 x < 0$ (see Proposition 2), we have $\psi'(x) < 0$ in $(0, +\infty)$ and it means that $\psi(x)$ is strictly decreasing on $[0, +\infty)$. Since $\psi(+\infty) = \lim_{x\to+\infty}\frac{1-x\coth x}{x} = -1$ and $\psi(0) = 0$, we obtain $-1 < \frac{1-x\coth x}{x} < 0$ in $(0, +\infty)$. (ii) Similarly, we have $0 < \frac{1-x\coth x}{x} < 1$ in $(-\infty, 0)$. □

References

[1] J. Bear, Dynamics of Fluids of Porous Media, American Elsevier Publishing Company, New York, 1972.
[2] G.Q. Chen, Z. Gao, Z.F. Yang, A perturbational h^4 exponential finite difference scheme for convection diffusion equation, J. Comput. Phys. 104 (1993) 129–139.
[3] M. Ciment, S.H. Leventhal, B.C. Weinberg, The operator compact implicit method for parabolic equations, J. Comput. Phys. 28 (1978) 135–166.
[4] W. Dai, R. Nassar, Compact ADI method for solving parabolic differential equations, Numer. Meth. Partial Differential Eq. 18 (2002) 129–142.
[5] D.N. de G Allen, R.V. Southwell, Relaxation methods applied to determine the motion in two dimensions of a viscous fluid past a fixed cylinder, Quart. J. Mech. Appl. Math. 8 (1955) 129–143.
[6] S.C.R. Dennis, Finite difference associated with second-order difference equations, Quart. J. Mech. Appl. Math. 13 (1960) 487–507.
[7] S.C.R. Dennis, J.D. Hudson, Accurate representations of partial differential equations by finite difference schemes, J. Inst. Math. Appl. 23 (1979) 43–51.
[8] S.C.R. Dennis, J.D. Hudson, Compact h^4 finite-difference approximations to operators of Navier–Stokes type, J. Comput. Phys. 85 (1989) 390–416.
[9] E.C. Gartland Jr., Uniform high-order difference schemes for a singularly value prob. Math. Comput. 48 (1987) 551–564.
[10] M.M. Gupta, R.P. Manohar, J.W. Stephenson, A single cell high order scheme for the convection–diffusion equation with variable coefficients, Int. J. Numer. Meth. Fluids 4 (1984) 641–651.
[11] R.S. Hirsh, Higher order accurate difference solutions of fluid mechanics problems by a compact differencing technique, J. Comput. Phys. 19 (1975) 90–109.
[12] J.C. Kalita, D.C. Dalal, A.K. Dass, A class of higher order compact schemes for the unsteady two-dimensional convection–diffusion equation with variable convection coefficients, Int. J. Numer. Meth. Fluids 38 (2002) 1111–1131.
[13] S. Karaa, J. Zhang, High order ADI method for solving unsteady convection–diffusion problems, J. Comput. Phys. 198 (2004) 1–9.
[14] M. Li, T. Tang, B. Fornberg, A compact fourth-order finite difference scheme for the incompressible Navier–Stokes equations, Int. J. Numer. Meth. Fluids 20 (1995) 1137–1151.
[15] R.J. MacKinnon, R.W. Johnson, Differential equation based representation of truncation errors for accurate numerical simulation. Int. J. Numer. Meth. Fluids. 13 (1991) 739–757.
[16] B.J. Noye, H.H. Tan, A third-order semi-implicit finite difference method for solving the one-dimensional convection–diffusion equation, Int. J. Numer. Meth. Eng. 26 (1988) 1615–1629.
[17] B.J. Noye, H.H. Tan, Finite difference methods for solving the two-dimensional advection–diffusion equation, Int. J. Numer. Meth. Fluids 9 (1989) 75–89.
[18] S.V. Patankar, Numerical Heat Transfer and Fluid Flows, McGraw-Hill, New York, 1980.
[19] D.W. Peaceman, H.H. Rachford Jr., The numerical solution of parabolic and elliptic differential equations, J. Soc. Ind. Appl. Math. 3 (1959) 28–41.

[20] A. Rigal, High order difference schemes for unsteady one-dimensional convection–diffusion problems, J. Comput. Phys. 114 (1994) 59–76.
[21] P.J. Roache, Computational Fluid Dynamics, Hermosa, Albuquerque, NM, 1976.
[22] D.F. Roscoe, New methods for the derivation of stable difference representations for differential equations, J. Inst. Math. Appl. 16 (1975) 291–301.
[23] A. Segal, Aspects of numerical methods for elliptic singular perturbation problems, SIAM J. Sci. Statist. Comput. 3 (1982) 327–349.
[24] D.B. Spalding, A novel finite difference formulation for differential equations involving both first and second derivatives, Int. J. Numer. Meth. Eng. 4 (1972) 551–559.
[25] W.F. Spotz, G.F. Carey, High-order compact scheme for the steady stream-function vorticity equations, Int. J. Numer. Meth. Eng. 38 (1995) 3497–3512.
[26] W.F. Spotz, G.F. Carey, Extension of high-order compact schemes to time-dependent problems, Numer. Meth. Partial Differential Eq. 17 (2001) 657–672.
[27] J.W. Thomas, Numerical Partial Differential Equations: Finite Difference Methods, Springer, New York, 1995.
[28] Z.F. Tian, Y.B. Ge, A fourth-order compact finite difference scheme for the steady streamfunction-vorticity formulation of the Navier–Stokes/Boussinesq equations, Int. J. Numer. Meth. Fluids 41 (2003) 495–518.
[29] J. Zhang, An explicit fourth-order compact finite difference scheme for three dimensional convection–diffusion equation, Commun. Numer. Meth. Eng. 14 (1998) 209–218.
[30] J. Zhang, Preconditioned iterative methods and finite difference schemes for convection–diffusion, Appl. Math. Comput. 109 (2000) 11–30.
[31] J. Zhang, Multigrid method and fourth order compact difference scheme for 2D Poisson equation unequal meshsize discretization, J. Comput. Phys. 179 (2002) 170–179.